Mobile Robot With Robotic Arm: Development and Validation of a Digital Twin

Proceedings of the ASME 2023
International Mechanical Engineering Congress and Exposition
IMECE2023
October 29-November 2, 2023, New Orleans, Louisiana

IMECE2023-113056

MOBILE ROBOT WITH ROBOTIC ARM: DEVELOPMENT AND VALIDATION OF A DIGITAL TWIN

Laura Salamina
Politecnico di Torino
Turin, Italy

Matteo Gaidano
Politecnico di Torino
Turin, Italy

Matteo Melchiorre
Politecnico di Torino
Turin, Italy

Stefano Mauro
Politecnico di Torino
Turin, Italy

ABSTRACT

Mobile robots coupled with robotic arms are a powerful instrument for factory automation, and they have become more and more popular in last years. Their digital twins allow to simulate the behavior in an industrial environment, increasing the capability to monitor their performance to detect failures or deviation from expected behavior. This work considers a system composed by a MiR250 mobile robot and by a UR5 anthropomorphic robot and describes the digital twin of the composed system. The digital twin is the coupling of the model of the UR5 robotic arm and that of the mobile robot. The model of the mobile robot considers a dynamic model of each wheel, to investigate the behavior of driving and caster wheels, and the model of the motors, to evaluate the expected motor torque. The digital twin of the UR5 robotic arm was tuned according to an identification methodology previously developed. An experimental campaign was carried using an Optitrack motion capture system. The results show that the model can provide reliable data to check and forecast the behavior of the system. The paper describes the complete model of the system, discusses its identification process, and shows some results obtained in the experimental campaign.

Keywords: digital twin, mobile robot, mobile manipulator, industrial robot.

1. INTRODUCTION

Mobile robots coupled with robotic arms are a powerful instrument for factory automation, and they have become more and more popular in last years. They can perform complex tasks such as manipulation, assembly, inspection, and transportation in various industrial scenarios. However, designing, testing, and controlling such systems pose significant challenges, as they involve multiple components, sensors, actuators, and interactions with the environment. In [1], the challenges and requirements for developing and applying autonomous industrial mobile manipulator systems are investigated, such as sustainability, configuration, adaptation, autonomy, positioning, manipulation and grasping, robot-robot interaction, human-robot interaction, process quality, dependability, and physical properties. [2] proposes an autonomous mobile manipulator that effectively overcomes inherent system uncertainties and exceptions by utilizing control strategies that employ coordinated control, combine visual and force servoing, and incorporate sophisticated reactive task control. In [3], instead, the coordinated motion of a mobile manipulator is planned, considering both stability and manipulation task, using a method based on the concept of valid stable region to evaluate stability in the presence of disturbances. Due to the complexity of the system, there is a need for effective tools and methods to simulate, monitor, and optimize the behavior and performance of mobile robot-arm systems. One promising approach is to use digital twins, which are virtual representations of physical systems that can mirror their states, properties, and dynamics in real time. Digital twins, as a new technology, can achieve semi-physical simulations that can save a lot of time and money for physical commissioning by finding design flaws early on [4,5]. The deployment of Digital Twin allows the production system to compensate the real-world uncertainty of the environment as well as of human behavior unpredictability. Thus, the need for offline programming and validation of robot motions when process changes are required is not needed, minimizing the needed time and effort [6]. In addition, they allow to reduce development costs and risks, improving operational efficiency and quality, enhancing fault detection and diagnosis, and supporting decision making and maintenance. However, developing accurate and reliable digital twins for mobile robot-arm systems is not trivial, as it requires modelling various aspects of the system at different levels of abstraction and fidelity, integrating heterogeneous data sources and formats, and validating the models against real-world measurements and

observations. An example of model of mobile manipulator is given in [7], where the equations of motion are derived using the Euler-Lagrange formulation for the nonholonomic model of the mobile manipulator. A similar approach is used in [8], where the dynamic model considers slip of the platform's tires using Dugoff's tire friction model.

In this paper, the digital twin of a system composed by a MiR250 mobile robot and by a UR5 anthropomorphic robot. The MiR250 is a compact and flexible mobile robot that can navigate autonomously in dynamic environments and carry payloads up to 250 kg. The UR5 is a lightweight and versatile collaborative robotic arm that can perform various manipulation tasks with high precision and repeatability. The combination of these two robots can enable a wide range of applications in factory automation, such as picking and placing objects, assembling parts, or inspecting products. Collaborative robots, or cobots, are a type of industrial robot that can interact directly with humans in a shared workspace. Cobots from Universal Robot (UR) are well-known and used a lot for collaborative applications. In [9,10] examples of hand-over between robot and human operator are shown, suggesting a possible experimental layout. UR robots are well-known both in industrial and research fields and their dynamic parameters for the evaluation of high-fidelity models have been investigated [11,12]. Since MiR250 is a relatively new mobile robot with limited material available, the work will concentrate on defining the model and estimating the parameters of the mobile robot. In [13], the model of a mobile manipulator, composed by a UR5 mounted on a MiR200, is developed using Lagrange formulation. In the present work, instead, the model is built exploiting the potentialities of Simscape Multibody toolbox, which allows to access to many data of the model. Moreover, Simulink offers the distinct advantage of facilitating comprehensive simulations that encompass a wide range of environmental elements. These simulations enable the integration of data from various sensors found in industrial environments, including the robot ones. The digital twin makes also possible to consider a human presence along the path, thus allowing for the simulation of task execution, collision avoidance, obstacle detection, and other critical aspects. Parameter estimation and model validation have been performed through an experimental campaign that records the motion of the UR5 end effector and the motion of the MiR250 base center with an Optitrack motion capture system. Optitrack is often used for tracking human body motion, as in [14] for collaborative robotic applications. In this application it is used as a high-precision measurement instrument for the motion of the robots.

2. ROBOTIC SYSTEM

The robotic system used for the development of the digital twin is composed of a UR5 e-series collaborative robot and a MiR250 mobile robot. In

FIGURE ***1*** a picture of the system is shown. As can be seen, a cabinet is placed between the two robots, in which the UR5 control unit is held. Here, the output pins of the MiR250 are connected with the input pins of the UR5, allowing the interaction between the two robots. MiR and UR companies collaborates in developing advanced robotic systems, so their products do not present compatibility issues.

2.1 UR5 Anthropomorphic Arm

UR5 anthropomorphic arm is a well-known 6-dof collaborative robot. It has a payload of 5 kg and a reach of 850 mm. Each joint can turn 360°, both clockwise and counterclockwise, with a maximum velocity of $180°/s$.

2.2 MiR250 Mobile Robot

MiR250 mobile robot is an Autonomous Mobile Robot (AMR), that uses laser scanners for spatial localization and obstacle detection. It can reach a maximum velocity of 2 m/s and has a payload of 250 kg. The positioning accuracy is 50 mm. The robot has 2 differential driving wheels and four caster wheels.

FIGURE 1: COMPLETE ROBOTIC SYSTEM

3. DIGITAL TWIN

The complete system has been described in a digital twin that includes the dynamic models of both the robots. The digital twin has been developed in Matlab/Simulink environment, using in particular, the Simscape Multibody toolbox. In the following, the model of the UR5 and the model of the MiR250 are presented, and then how the two models are merged.

3.1. UR5 numerical model

The model of UR5 collaborative robot has been developed in Simulink, using Simscape multibody toolbox, and it is based on the model developed by Raviola [11,12] and has been already validated alone. The model includes the significative elements of the robot. The main scheme is shown in **Errore. L'origine riferimento non è stata trovata.**.

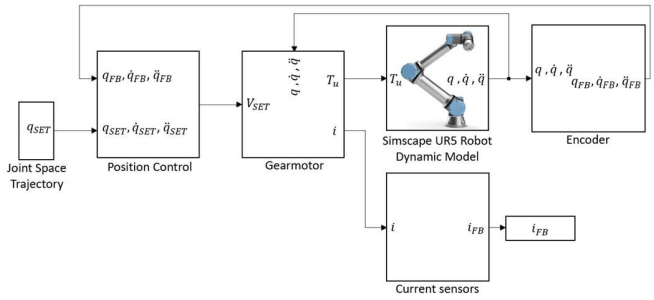

FIGURE 2: DYNAMIC MODEL OF UR5 ROBOT

As can be seen, the model is composed of the block relative to the set trajectory expressed in joint space, the position control block, the gearmotor model block, the dynamic model of the joints of the robot, and sensor blocks, relative to current sensors and encoders. The Joint Space Trajectory subsystem refers to the set values of angular position q_{SET}, velocity $\dot{q}_{SET}$ and acceleration $\ddot{q}_{SET}$ of all the six joints of the robot. These values are input of the Position Control block, where the control system of each joint is defined.

The Position Control applies a PID control algorithm to the error between set and feedback position. The feedback position is calculated in the Dynamic Model Block of the robot. The output is the set voltage V_{SET} of each joint motor, that enters the Gearmotor block. Besides voltage, the angular velocity values of the joints of the robot enters the block, too. Gearmotor block is divided into model of the motors and model of the gearbox, for all the joints of the robot. The motors are modelled as DC motors, with the RL-circuit equations. The data of the motors are taken from the datasheet of the motors. The gearboxes are modelled as a gain, that expresses the reduction ratio and the efficiency of the relative gearbox. The block returns the value of the torques of the six joints. In FIGURE 3 the dynamic model of the UR5 developed in Simscape is shown. In Simscape, the kinematic chain of the joints has been recreated, inserting rigid bodies, complete with mass and center of mass information, joints, and translations. On the left, three fundamental blocks for solving Simscape systems have been inserted. A Weld Joint block allows you to insert an interlocking joint between the robot support flange and the ground.

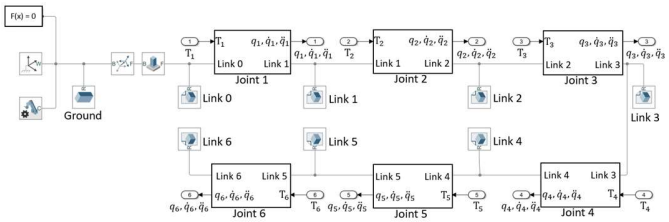

FIGURE 3: DYNAMIC MODEL OF ROBOT JOINTS

Referring to FIGURE 3, the information about mass, center of mass and geometry of the links of the robot are inside the Link blocks in the model, as well as the CAD of the link. The geometrical relations between a joint and the following one are expressed inside the Joint blocks and are expressed using the Denavit-Hartenberg DH convention. DH parameters, masses, center of masses and CADs are provided by Universal Robots [15] and they can be better identified as described in [11] . A revolute joint block is placed on the z_i axis of the i^{th} joint, and it has the torque T_i as input, and the value of angular position, angular velocity, and angular acceleration as output. In the end, in the Encoders block a unity gain is implemented for each joint, while in the Current Sensors block a first order transfer function is implemented for all the joints, in order to ensure a cutoff frequency of 2000 Hz.

3.2. MiR250 numerical model

The dynamic model of the MiR250 has been developed using Simscape multibody, too. In FIGURE 4 the architecture of the model is shown. A 6–DOF joint is present, to allow the robot to move freely in the space. Then, a Rigid Transform block is used to place the robot in a desired position in the simulation space. In particular, position and orientation of the robot depends on the starting position of the robot in the experimental tests.

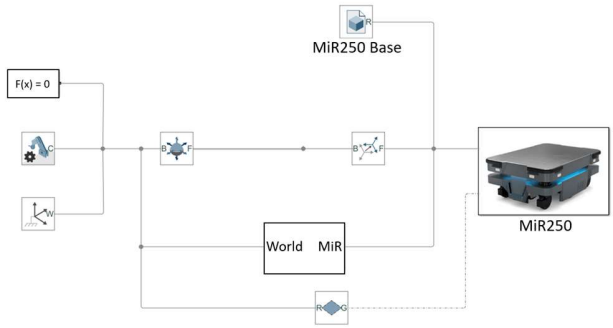

FIGURE 4: DYNAMIC MODEL OF MiR250 MOBILE ROBOT

The geometrical information of the robot has been evaluated from the relative CAD, available on [16]. The reference frame $o - xyz$ of MiR250 model is oriented as the one of the real robot: x–axis in the motion direction, z–axis on the vertical direction, pointing upward, and y–axis given by the right-hand rule. MiR250 base block involves the body of the robot, except for the six wheels and of the two motors. Since the robot is symmetric, the mass has been considered uniformly distributed. In the subsystem World-MiR the position sensors between the center of mass of the MiR, in position [0,0] in the $o - xyz$ reference frame, and the world reference frame $O - XYZ$ are defined, and they allow to obtain the position X and Y and the orientation Φ of the MiR250 during the simulations. The block at the bottom is an infinite virtual plane and is used to model the floor. In MiR250 block, the dynamic model of the robot, with the positioning of the six wheels with respect to the body of the robot and the control system, is built.

The control system is shown in FIGURE 5.

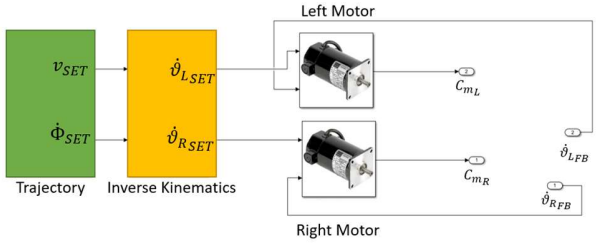

FIGURE 5: CONTROL SYSTEM OF MiR250 MODEL

On the left, the subsystem Trajectory reads, from the main program, the values of the SET linear velocity and of the SET angular velocity of the mobile robot during the simulation. The velocities are the linear velocity $\dot{X}$ of the MiR250 along X–

direction, the linear velocity $\dot{Y}$ of the MiR250 along Y–direction, and the angular velocity $\dot{\Phi}$, around the Z–axis.

The velocity values are input of the Inverse Kinematics subsystem, where it is possible to pass from velocity expressed in the World reference frame in the angular velocity of the differential driving wheels. The relationship between this information is expressed by:

$$\begin{Bmatrix} \dot{\vartheta}_r \\ \dot{\vartheta}_l \end{Bmatrix} = \frac{1}{r} \begin{bmatrix} \cos\varphi & \sin\varphi & a \\ \cos\varphi & \sin\varphi & -a \end{bmatrix} \begin{Bmatrix} \dot{X} \\ \dot{Y} \\ \dot{\varphi} \end{Bmatrix} \quad (1)$$

in which $\dot{\vartheta}_r$ and $\dot{\vartheta}_l$ are the angular velocity of the right and of the left wheel, respectively, r is the radius of the driving wheels and a is the wheelbase between the driving wheels. The SET values of the velocity of the wheels, times the reduction ratio of the gearbox, are inputs of the Left Motor and Right Motor subsystems, which contain both the control system and the motor model. A speed control is used, with two nested control loops, the outermost speed and the innermost current. Both use a PID control algorithm. The motors are modelled as DC motors. The output is the value of the torque of the motors. In FIGURE 6, the dynamic model of the driving wheel is presented, using the left one as reference. The Rigid Transform allows to position the wheel, with respect to the mobile robot, in the proper position.

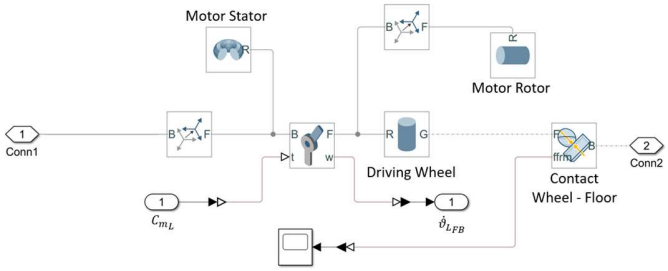

FIGURE 6: DRIVING WHEEL DYNAMIC MODEL

A revolution solid represents the stator of the motor. Then, the Revolute Joint is inserted, which allows the rotation of the driving wheel. The joint has a rotational degree of freedom, aligned along the z–axis. The joint determines the motion of the wheel by accepting as input the torque value calculated in the motor model. In output, it returns the value of the angular speed of the joint itself, and therefore of the wheel coupled to it. The rotor of the motor is inserted in cascade to the joint since the inertia of the rotor must be related to the revolute joint of the wheel. Finally, the driving wheel is connected to the rotary joint. The geometry of the wheel is known, and the mass is estimated using the density of the polyurethane. The block Contact Wheel-Floor allows to define the contact between the wheel and the virtual plane. The normal force is described as a spring-damper system, and the frictional force is modelled as a stick-slip.

In FIGURE 7, instead, the dynamic model of the front left caster wheel is shown. Each caster wheel has two Revolute Joints, the first for the rotation of the pivot that supports the wheel, therefore rotating around the vertical direction, and the second for the rotation of the wheel itself, like driving wheels. The motion of the joints is determined by the effect of frictional forces on the wheels. Also in this case, the first block of Rigid Transform is dedicated to the correct positioning of the caster wheel system. The first Revolute Joint is then inserted, for which a damping coefficient is specified. A subsequent transformation allows to position the pivot of the wheel in the correct way, in the Pivot block. Here, the CAD file of the pivot is recalled, and the density of the steel and a uniformly distributed mass are assigned to it. Another Rigid Transform allows to correctly position the joint related to the rotation of the wheel. The caster wheel is connected to the Revolute Joint, specifying its density and a uniform mass distribution. The Contact Wheel-Floor block is used to model the contact forces, normal and friction ones, between the wheel and the virtual plane.

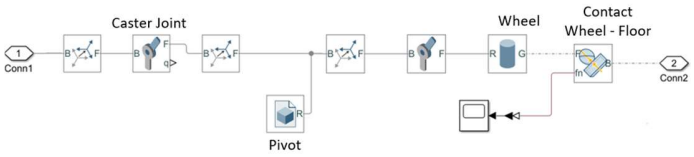

FIGURE 7: CASTER WHEEL DYNMIC MODEL

Unfortunately, little information was available for the realization of the model. The data relative to the electric circuit of the motors are given by the manufacturer. The missing data have been derived comparing the data available with those of commercial motors with similar characteristics. From the CAD drawing of MiR250 [16], the distances between the wheel axles, the height of the wheel centers from the ground and the height of the centering of the casters from the ground have been identified. In this way, it is possible to reconstruct the kinematics of the robot. The dimensions of the six wheels have been determined. The density of the wheels is assumed equal to that of polyurethane, and the mass is uniformly distributed. The geometry of the pivot has been identified from the CAD, the density is assumed equal to that of steel and the mass uniformly distributed. The values of the static and dynamic friction coefficient have been then identified. The initial data used for the MiR250 model are shown in TABLE 1. As shown in section 5, the most relevant parameters have been adjusted with the Simulink Optimization Toolbox using experimental trajectories.

TABLE 1: INITIAL DATA OF MiR250 MODEL

Available Data	
Total Mass MiR250 [kg]	83
Height MiR [m]	0.300
Length MiR [m]	0.800
Width MiR [m]	0.580
Driving wheel diameter [m]	0.200
Caster wheel diameter [m]	0.125
Driving wheel axis, along y [m]	0.410
Caster wheel axis, along y [m]	0.375
Caster wheel axis, along x [m]	0.500
Reduction ratio [-]	10.167
Nominal current [A]	20.7

Torque constant [Nm/A]	0.15
Estimated Data	
Wheel density [kg / m^3]	100
Wheel joint damping [N*m/(rad/s)]	1e-5
Static friction coefficient [-]	0.5
Dynamic friction coefficient [-]	0.3
Contact stiffness [N/m]	1e6
Contact damping [N/(m/s)]	1e3
Motor nominal velocity [rad/s]	250
Motor nominal torque [Nm]	2.25
Motor circuit time constant [s]	1e-3
Motor mass [kg]	3
Rotor mass [kg]	1.5
Rotor diameter [m]	0.100
Current loop crossover frequency [rad/s]	2000π
Current loop PID Proportional	20
Current loop PID Integrative	5
Current loop PID Derivative	0
Velocity loop crossover frequency [rad/s]	200π
Velocity loop PID Proportional	20
Velocity loop PID Integrative	0.01
Velocity loop PID Derivative	0
Motor maximum acceleration [rad/s^2]	1822
Velocity loop phase margin [°]	87

3.3 Complete system digital twin

The digital twin of the robotic system under study has been developed combining the models of the UR5 and of the MiR250. As can be seen in

FIGURE ***1***, the UR5 leans on a cabinet, placed on the mobile robot base, inside which the robot control unit is placed. Therefore, the presence of the cabinet in the model has been considered, too. In FIGURE 8, the digital twin of the complete model is shown.

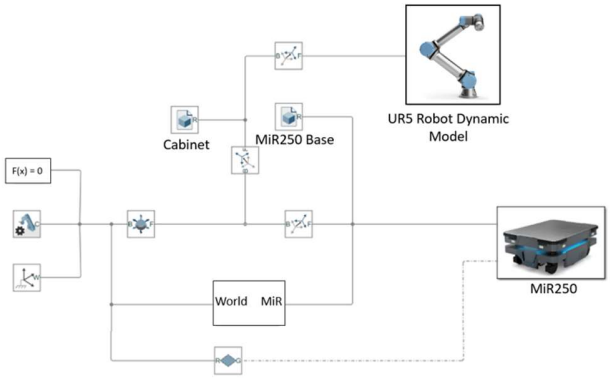

FIGURE 8: COMPLETE SYSTEM DIGITAL TWIN

As can be seen, the digital twin preserves the structure of the mobile robot model, and it adds the contribution of the cabinet, that is placed on the MiR250 base using a Rigid Transformation, and the contribution of the UR5. In the subsystem UR5 Robot Dynamic Model, the complete model of the robot, as explained in section 3.1. The CAD file of the cabinet and the complete system of

FIGURE ***1*** has been provided. The coordinates of the positioning point of the robot on the cabinet were extracted from the CAD of the complete system. The mass of the cabinet, with the control unit, is equal to 15 kg. The acquired data for the MiR250 are odometric feedback obtained through rest APIs, i.e., position and speed, and position measurements performed using the Optitrack vision system. The acquired data for the UR5, instead, are the joint velocities of the six joints and the position of the end effector of the robot using the Optitrack vision system. The digital twin reads as input the joint velocity of the UR5 and the velocity of the MiR250 acquired from rest APIs.

The resulting 3D model in Simscape Multibody is shown in FIGURE 9.

FIGURE 9: GRAPHIC REPRESENTATION OF THE MODEL BY SIMSCAPE MULTIBODY

4. LABORATORY SETUP

The experimental set-up is shown in

FIGURE ***10***. The area is observed by an Optitrack vision system equipped with 4 cameras, identified with O1, O2, O3 and O4. The vision system is based on the tracking of passive markers and can measure their position with an error of 0.5 mm.

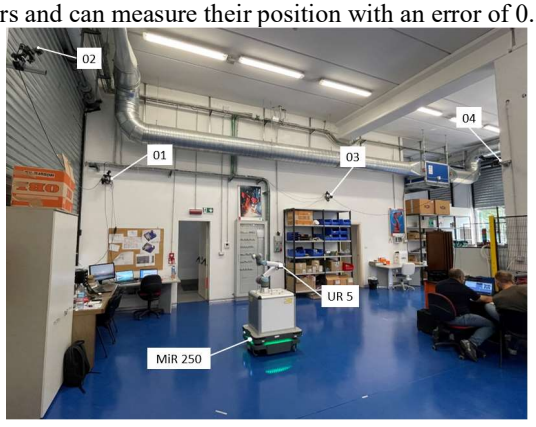

FIGURE 10: LABORATORY SETUP

By appropriately placing at least three markers on each part of interest, it is possible to measure the position and the orientation of that body. In this work, the markers have been applied to track the pose of the MiR and of the end-effector of the robotic arm, as shown in FIGURE 11.

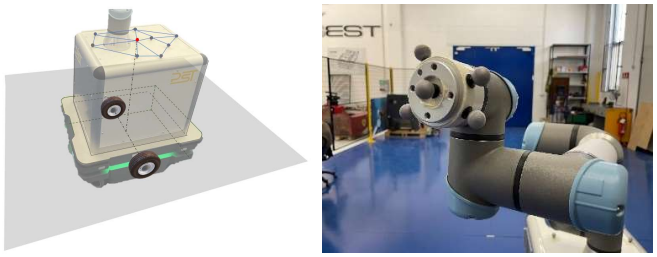

FIGURE 11: MARKER POSITIONS FOR TRACKING OF SIGNIFICANT PARTS

The layout is schematized in FIGURE 13. The Optitrack measurements are provided in the $O-xyz$ reference system, obtained during the calibration procedure of the 4 cameras. The feedback data of the mobile robot, instead, are retrieved with respect to the MiR frame $O-x_My_Mz_M$. These two reference frames usually do not coincide. For example, in the case of this work, the MiR frame was actually out of the field of view of Optitrack, as it was defined during the first mobile robot software setup by the manufacturer. The comparison of the data coming from the various sensors is possible following the spatial calibration procedure, which consists in finding the matrix that allows to transform the data acquired by MiR in the Optitrack reference system. For this purpose, it is sufficient that the positions of three points are known in the reference systems $O-xyz$ and $O-x_my_mz_m$. In practice, Optitrack markers are placed on the upper face of the box on which the UR5 base is mounted. Markers are arranged to create an asymmetrical geometry that is easily recognized by Optitrack. These markers define a rigid body to which the MiR pose is associated. In particular, the position of the MiR is defined by the marker which, considering the projection of the robot onto the support surface, identifies the center line of the drive wheels (FIGURE 11). Through its own navigation interface, the MiR is then moved to three different points, denoted as A, B and C in FIGURE 12 and FIGURE 13, whose poses are recorded both by Optitrack and rest API. An auxiliary reference frame $O_a-x_ay_az_a$ is defined, to identify the relationship between $O-x_my_mz_m$ and $O-xyz$. The desired transformation matrix $\boldsymbol{A}_m^o$ can be calculated as $\boldsymbol{A}_m^o = \boldsymbol{A}_a^o(\boldsymbol{A}_a^m)^{-1}$, in which $\boldsymbol{A}_a^o$ is the transformation matrix between the auxiliary system and the Optitrack system and $\boldsymbol{A}_a^m$ is the transformation between the auxiliary reference frame and the MiR reference frame. Being $\mathbf{p}_A^o$, $\mathbf{p}_B^o$ e $\mathbf{p}_C^o$ the position column vectors of A, B and C in $O-xyz$, the matrix $\boldsymbol{A}_a^o$ is calculated as:

$$\boldsymbol{A}_a^o = \begin{vmatrix} \hat{\boldsymbol{x}}_a^o & \hat{\boldsymbol{y}}_a^o & \hat{\boldsymbol{z}}_a^o & \boldsymbol{p}_A^o \\ 0 & 0 & 0 & 1 \end{vmatrix}, \quad (2)$$

$$\hat{\boldsymbol{x}}_a^o = (\boldsymbol{p}_B^o - \boldsymbol{p}_A^o)/\|\boldsymbol{p}_B^o - \boldsymbol{p}_A^o\|, \quad (3)$$

$$\hat{\boldsymbol{z}}_a^o = [(\boldsymbol{p}_B^o - \boldsymbol{p}_A^o) \times (\boldsymbol{p}_C^o - \boldsymbol{p}_A^o)]/\|(\boldsymbol{p}_B^o - \boldsymbol{p}_A^o) \times (\boldsymbol{p}_C^o - \boldsymbol{p}_A^o)\|, \quad (4)$$

$$\hat{\boldsymbol{y}}_a^o = \hat{\boldsymbol{z}}_a^o \times \hat{\boldsymbol{x}}_a^o, \quad (5)$$

with $\hat{\boldsymbol{x}}_a^o$, $\hat{\boldsymbol{y}}_a^o$ and $\hat{\boldsymbol{z}}_a^o$ the versors of $O_a-x_ay_az_a$ in Optitrack reference frame. The same holds for $\boldsymbol{A}_a^m$. In FIGURE 12 the necessary reference frames and position vectors are represented. With this information, the matrix $\boldsymbol{A}_m^o$ can be calculated, and the recorded data can all be expressed in the Optitrack reference frame.

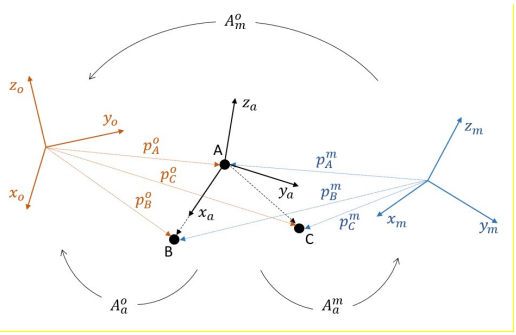

FIGURE 12: REFERENCE SYSTEM TRANSFORMTION FROM MIR TO OPTITRACK ONE, WITH THE AUXILIARY REFERENCE FRAME

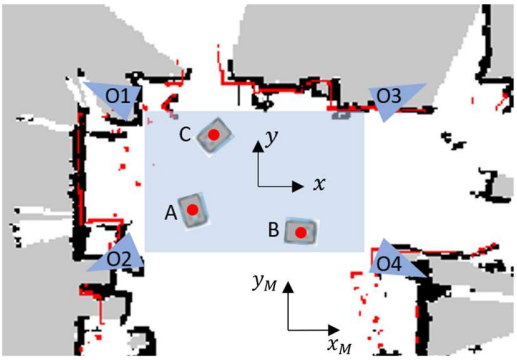

FIGURE 13: 2D MAP OF THE LABORATORY. THE SHADED RECTANGLE IS THE REGION COVERED BY THE OPTITRACK SYSTEM.

5. RESULTS

5.1 Reference trajectories

Two types of trajectories of the mobile robot were considered for the tuning and validation of the model. The first class of trajectories is denoted with the letter "I" and is characterized by almost straight paths. The second family of trajectories consists of arc paths and is referred to by the abbreviation "C". The start and end points of the mission are chosen appropriately using the navigation software. To obtain the trajectories C, inaccessible areas have been set up through the MiR software to drive the AGV along a curve, as shown on the right in FIGURE 14. In TABLE 2 are shown the data that have been used for identification and validation of the model. For each test, the following data have been acquired:

- Trajectory of MiR and of the end-effector of the UR5, measured by Optitrack, in terms of position and orientation.
- Trajectory of MiR and of the end-effector of the UR5, provided by data feedback of the respective software, in terms of position and orientation
- Speed set from MiR software.

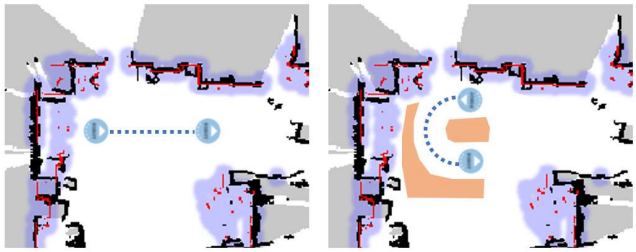

FIGURE 14: STRAIGHT (LEFT) AND CURVED (RIGHT) TRAJECTORIES DEFINED FROM THE MIR SOFTWARE INTERFACE

TABLE 2: TYPES OF TRAJECTORIES USED FOR PARAMETERS ESTIMATION AND MODEL VALIDATION

Test	Trajectory Type	UR5 motion (Y=yes, N=No)	Purpose
IN1	I	N	Identification
IN2	I	N	Identification
CN1	C	N	Identification
CN2	C	N	Validation
CY	C	Y	Validation
IY	I	Y	Validation

5.2 Parameters estimation

To identify some of the dynamic parameters of the AGV not given by the manufacturer, a tuning was carried out with respect to measured trajectories. When possible, parameters have been calculated from available data. For instance, masses were deduced from the geometry of the available drawings and from these a first attempt value was chosen. The control parameters were initially estimated using the Simulink PID tuner, but a second analysis was deemed appropriate during the optimization phase. TABLE 3 shows the parameters under examination.

The Parameter Estimator provided in the Simulink Design Optimization Toolbox was used to optimize the model based on the experimental data [17]. The optimization problem is built based on tests IN1, IN2 and CN1. As parameters to be estimated for the MiR, the estimation set considers the UR5 not moving. For each trial, the model receives as input the speed set experimentally acquired by MiR via rest API and the result is compared with the experimental trajectory, expressed in terms of position (x,y coordinates) and orientation (Φ). The cost function is defined by the Parameter Estimator tool considering the sum squared error between the model trajectory and the Optitrack measurements.

First, a sensitivity analysis was performed to understand which of the estimated parameters had the greatest impact on the response of the model. The sensitivity analysis is conducted by generating random values according to a uniform distribution in a range compatible with the initial estimate. In the specific case, 20 different sets of the parameters in TABLE 3 are considered and the resulting error is calculated for each one. The most influent parameters are identified through a statistical analysis, reported in the diagrams in FIGURE 15 in the form of tornado plots. The Parameter Influence statistical index is a value between -1 and 1 that is computed by correlation method [18]. A high value indicates how much the parameter affects the model's response with respect to the experimental data. The sign, on the other hand, indicates whether an increase in the parameter corresponds to an increase or a decrease of the error. It can be observed that for each test the four most influential parameters are the friction coefficients f and f_a, the control constant K_i and the mass of the rotors m_{rotor}. Therefore, it was chosen to perform a tuning of these four parameters, given the limited influence of the others. This allows to significantly reduce the calculation times. Moreover, it was observed that even increasing the number of parameters to be estimated, results did not change significantly.

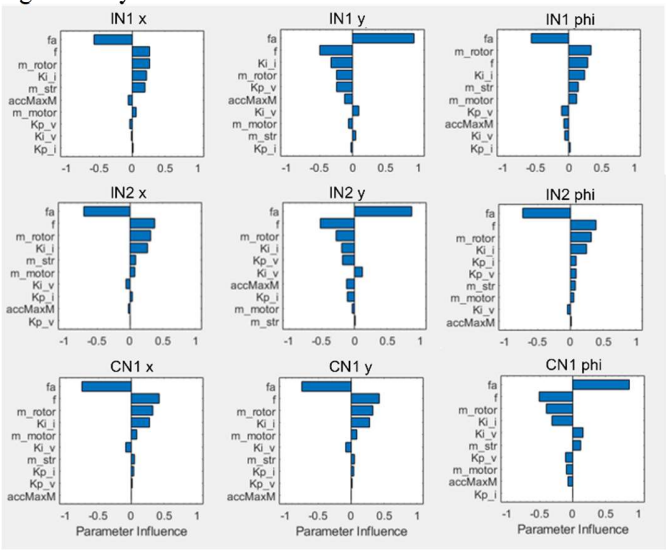

FIGURE 15 ANALYSIS OF THE INFLUENCE OF THE MODEL PARAMETERS ON THE MODEL RESPONSE

TABLE 3 PARAMETERS CONSIDERED FOR SENSITIVITY ANALYSIS AND ESTIMATION

Parameter	Description	Init. value	Opt.
f	Dynamic friction coeff.	0.30	0.48
f_a	Static friction coeff.	0.50	0.53
m_{str}	Mass of the control box	15 kg	-
Ki_i	Integrative gain (current loop)	5	5.5
Ki_v	Integrative gain (velocity loop)	0.01	-
Kp_i	Proportional gain (current loop)	20	-
Kp_v	Proportional gain (velocity loop)	20	-
acc_{maxM}	Max acceleration of the motor	1822 rad/s^2	-
m_{motor}	Mass of the motor	3 kg	-
m_{rotor}	Mass of the rotor	1.5 kg	1.62

For each trial, velocity inputs are provided to the model and the parameter estimator varies the parameters so as to minimize the cost function, constructed as the sum of the squared errors of all the trials (in the present case IN1, IN2 and CN1). FIGURE 16 shows the result of the optimization. Only one test is reported as results are very similar for the tests of the estimation set. The values of the optimized parameters are reported in TABLE 3.

As can be seen, the model follows the experimental trajectory well in x and φ, while there remains a small discrepancy along y, even after several fitting attempts. This indicates the possibility to improve the model in the future, for example by a more precise modeling of the caster wheels that consider friction on the joints.

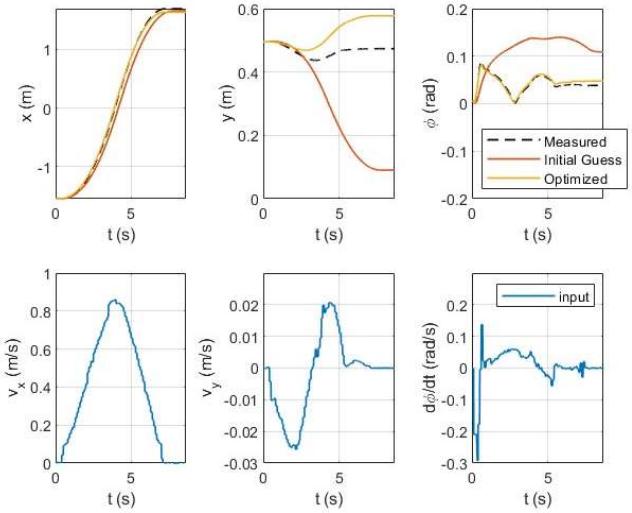

FIGURE 16: OPTIMIZATION OF TEST IN1

5.3 Model validation

The model is validated on the base of the three validation tests, two of which considering the UR5 moving. In the latter, to appreciate disturbances of the motion of the robotic arm on the mobile robot, the UR5 robot is positioned cantilevered from the support surface and it is activated by moving the first joint, so as to generate arc-shaped trajectories of the end-effector (FIGURE 17).

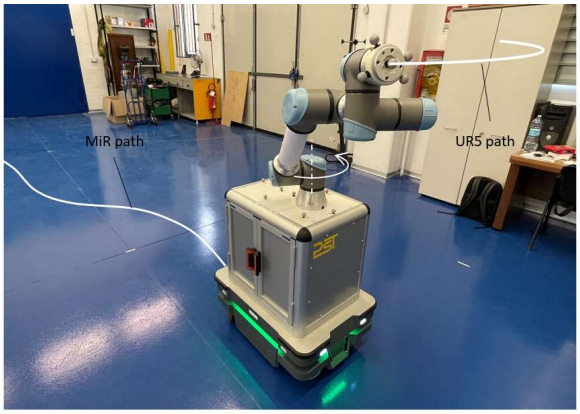

FIGURE 17: COMBINATION OF THE MOTION OF MOBILE ROBOT AND MANIPULATOR

To synchronize the movement of the UR5 robot within the MiR mission time frame, the UR5 program written in Polyscope waits for an input from the MiR mobile robot; when the input is read, the program starts the cyclic movement defined. As the test starts, the MiR sends this digital output to actuates the robotic arm. In this way the two robots are synchronized during data acquisition. FIGURE 18 shows two examples of trajectories where the arm moves.

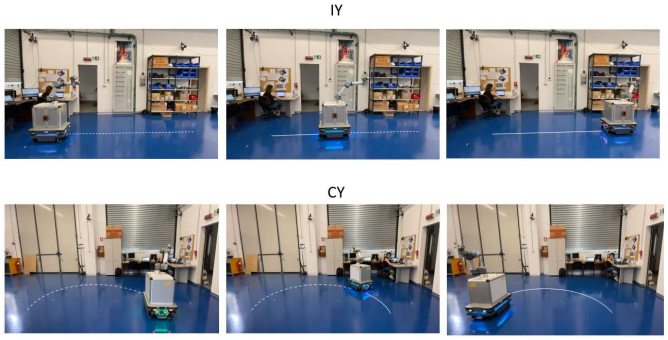

FIGURE 18: EXAMPLES OF IY AND CY TRAJECTORY TYPES

To validate the integrated model, the MiR is simulated giving as input the velocity set acquired experimentally, while the robotic arm is driven with the trajectories in the joint space acquired by the UR5. In this way the reaction at the base of the UR5, which constitutes a disturbance for the MiR control, will be the same as in the laboratory tests. This makes it possible to evaluate whether the behavior of the mobile base in the presence of disturbance due to the collaborative robot is comparable with that found experimentally. For validation, the Optitrack measurements are compared with the model output. For illustrative purposes, two examples of simulations are shown in FIGURE 19.

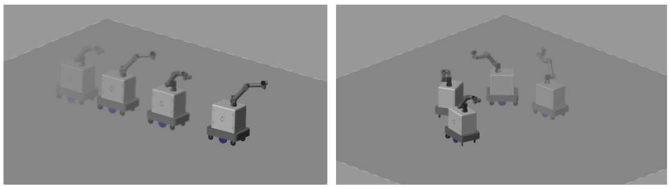

FIGURE 19: SIMULATION OF IY AND CY TRAJECTORIES

FIGURE 20 shows the results of the CN2 trajectory. In this case the UR5 is steady so only the MiR trajectory is reported. The simulation output matches measured data with a small error. Similar results are obtained when the robotic arm moves. FIGURE 21 and FIGURE 22 show the result of IY test in terms of trajectories. In particular, FIGURE 21 shows the trajectory of the mobile base. Observing the y_{MiR} and φ_{MiR} components, it can be seen that the model is affected by the oscillations due to the movement of the UR5, with a minimal error compared to the experimental measurements. The trajectory of the UR5 end-effector is shown in FIGURE 22. In the latter, the missing part of the dashed curves is due to the loss of Optitrack data. In fact, in the final part of the trajectory, the mobile robot stops close to the border of the Optitrack field of view and the end-effector of the UR5 exits the volume detected by the cameras because it is

extended. In test CY, the results of which are shown in FIGURE 23 and FIGURE 24, a different behavior of the mobile base is observed. This, in fact, does not seem to be affected by the movement of the UR5. The oscillatory behavior on x_{MiR}, y_{MiR} and φ_{MiR} is not evident. What is obtained is in line with the experimental results.

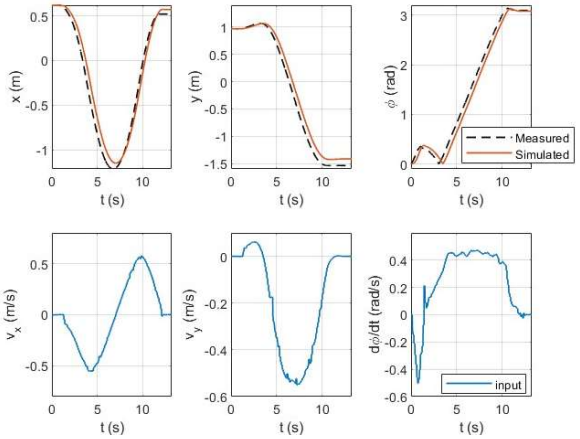

FIGURE 20: RESULTS OF TEST CN2

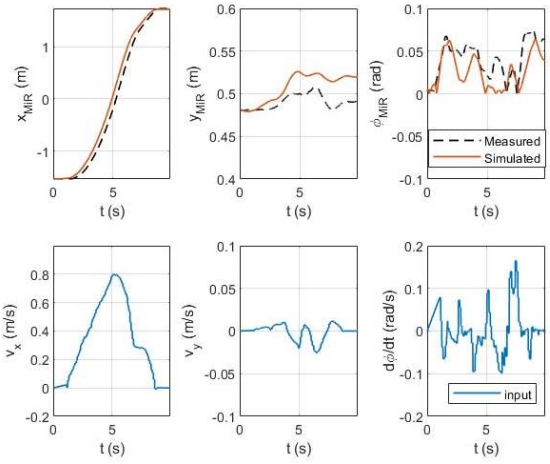

FIGURE 21: RESULTS OF EST IY - MIR TRAJECTORY

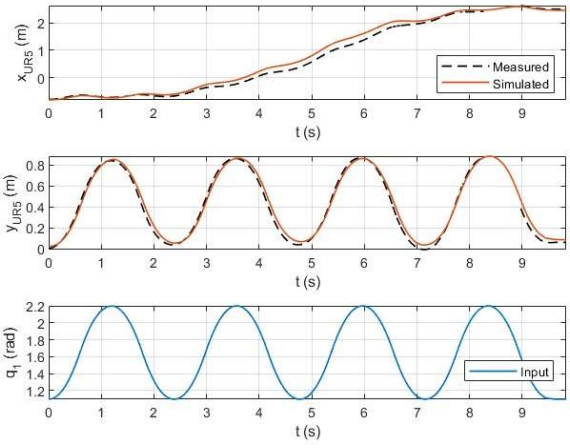

FIGURE 22: RESULTS OF EST IY – UR5 TRAJECTORY

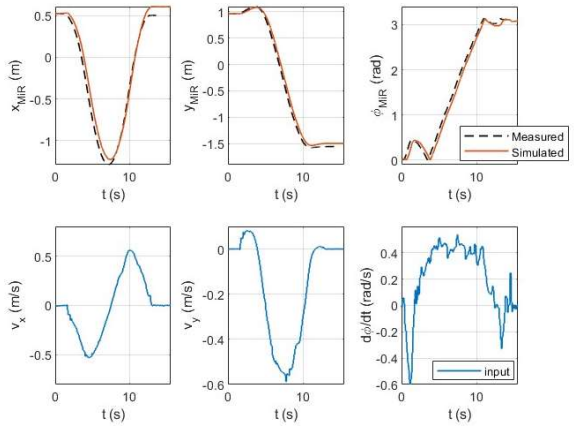

FIGURE 23: RESULTS OF EST CY - MIR TRAJECTORY

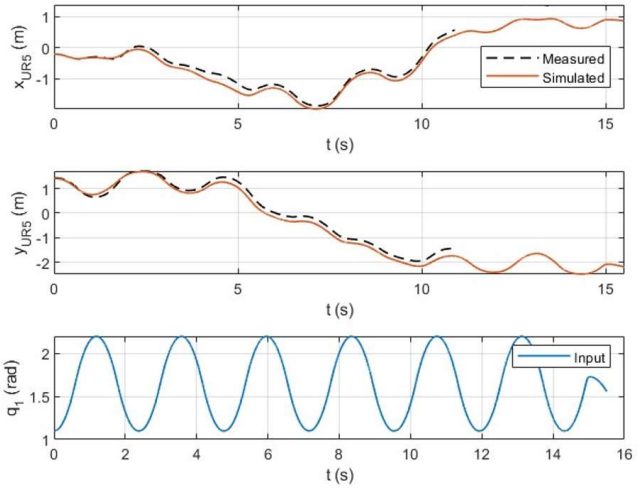

FIGURE 24: RESULTS OF EST CY – UR5 TRAJECTORY

6. CONCLUSION

The measurements carried out on the trajectories of the real system show that the proposed model and the procedure applied to identify its unknown parameters made possible to obtain an optimal fit between simulated and acquired data.

The model is mature enough to be used as a simulation instrument for testing human-robot interaction in industrial application. This can help in preliminary safety evaluation in order to reduce risks in real world scenario.

The model makes also disposable data about torque applied by the motors and the command signal computed by the motor controllers. In the future development of this work motor current to and angular velocity of the traction wheels will be measured and used as an input to the model in order, together with currents in the UR5 motors. This will make it possible to forecast the trajectory of the robot independently on its navigation sensors.

The digital twin is also an instrument that can be applied to different applications, including the survey of the system and the detection of possible failures.

ACKNOWLEDGEMENTS

The authors thank PST SRL of Turin (I) and TWM srl for their support in the development of this research.

REFERENCES

[1] Hvilshøj, M., Bøgh, S., Nielsen, O. S., and Madsen, O., 2012, "Autonomous Industrial Mobile Manipulation (AIMM): Past, Present and Future," Ind. Rob., **39**(2), pp. 120–135.

[2] Hamner, B., Koterba, S., Shi, J., Simmons, R., and Singh, S., 2010, "An Autonomous Mobile Manipulator for Assembly Tasks," Auton. Robots, **28**(1), pp. 131–149.

[3] Huang, Q., Tanie, K., and Sugano, S., 2000, "Planning for a Mobile Manipulator Considering Stability," pp. 732–742.

[4] Leng, J., Wang, D., Shen, W., Li, X., Liu, Q., and Chen, X., 2021, "Digital Twins-Based Smart Manufacturing System Design in Industry 4.0: A Review," J. Manuf. Syst., **60**(March), pp. 119–137.

[5] Lo, C. K., Chen, C. H., and Zhong, R. Y., 2021, "A Review of Digital Twin in Product Design and Development," Adv. Eng. Informatics, **48**(July 2020).

[6] Kousi, N., Gkournelos, C., Aivaliotis, S., Giannoulis, C., Michalos, G., and Makris, S., 2019, "Digital Twin for Adaptation of Robots' Behavior in Flexible Robotic Assembly Lines," Procedia Manuf., **28**, pp. 121–126.

[7] Varela-Aldas, J., Andaluz, V. H., and Chicaiza, F. A., 2018, "Modelling and Control of a Mobile Manipulator for Trajectory Tracking," Proc. - 3rd Int. Conf. Inf. Syst. Comput. Sci. INCISCOS 2018, **2018**-**Decem**, pp. 69–74.

[8] Chung, J. H., and Velinsky, S. A., 1998, "Modeling and Control of a Mobile Manipulator," Robotica, **16**(6), pp. 607–613.

[9] Melchiorre, M., Scimmi, L. S., Mauro, S., and Pastorelli, S. P., 2021, "Vision-Based Control Architecture for Human–Robot Hand-over Applications," Asian J. Control, **23**(1), pp. 105–117.

[10] Scimmi, L. S., Melchiorre, M., Mauro, S., and Pastorelli, S., 2019, "Experimental Real-Time Setup for Vision Driven Hand-Over with a Collaborative Robot," 2019 Int. Conf. Control. Autom. Diagnosis, ICCAD 2019 - Proc.

[11] Raviola, A., De Martin, A., Guida, R., Pastorelli, S., Mauro, S., and Sorli, M., 2021, "Identification of a UR5 Collaborative Robot Dynamic Parameters," Mech. Mach. Sci., **102**, pp. 69–77.

[12] Raviola, A., Guida, R., De Martin, A., Pastorelli, S., Mauro, S., and Sorli, M., 2021, "Effects of Temperature and Mounting Configuration on the Dynamic Parameters Identification of Industrial Robots," Robotics, **10**(3).

[13] Zhou, Z., Yang, X., Wang, H., and Zhang, X., 2022, "Digital Twin with Integrated Robot-Human/Environment Interaction Dynamics for an Industrial Mobile Manipulator," Proc. - IEEE Int. Conf. Robot. Autom., pp. 5041–5047.

[14] Palmieri, P., Melchiorre, M., Scimmi, L. S., Pastorelli, S., and Mauro, S., 2021, *Human Arm Motion Tracking by Kinect Sensor Using Kalman Filter for Collaborative Robotics*, Springer International Publishing.

[15] universal robots, 2022, "DH Parameters for Calculations of Kinematics and Dynamics" [Online]. Available: https://www.universal-robots.com/articles/ur/application-installation/dh-parameters-for-calculations-of-kinematics-and-dynamics/. [Accessed: 27-Apr-2023].

[16] klain robotics, "Klain Robotics Area Riservata" [Online]. Available: https://www.klainrobotics.com/area-riservata/.

[17] MathWorks, 2023, "Simulink Parameter Estimator" [Online]. Available: https://it.mathworks.com/help/sldo/ref/parameterestimator-app.html. [Accessed: 27-Apr-2023].

[18] MathWorks, 2023, "Sensitivity Analyzer" [Online]. Available: https://it.mathworks.com/help/sldo/ref/sensitivityanalyzer-app.html. [Accessed: 27-Apr-2023].